nature geoscience

Supporting Information for

Why increases in CO_2 cool the stratosphere and how this amplifies radiative forcing

Sean Cohen, Robert Pincus, Lorenzo Polvani

Sean Cohen.
E-mail: sean.cohen@columbia.edu

This PDF file includes:

Supporting Information Text

1. Why tropospheric cooling by CO_2 does not change with CO_2 concentration

When atmospheric CO_2 increases in the absence of any changes in column temperature, the longwave heating rate due to CO_2 changes non-uniformly along the atmospheric column. In the middle and upper stratosphere, the spectrally-integrated heating rate due to CO_2 (H_{CO_2}) increases sharply when CO_2 is quadrupled from preindustrial levels (Fig. S1, right), causing the stratosphere to cool at these pressure levels. In the troposphere and lower stratosphere, however, the spectrally-integrated heating rate due to CO_2 is almost entirely insensitive to changes in CO_2 concentration. This not only causes CO_2-induced stratospheric cooling to vanish in the lower stratosphere, but also causes longwave cooling by CO_2 in the troposphere to be insensitive to changes in CO_2 concentration (so long as surface temperature and, by extension, tropospheric temperature remain fixed).

This insensitivity of H_{CO_2} in the troposphere can be explained by the distribution of CO_2's mass absorption coefficients. Near present-day concentrations of CO_2, tropospheric cooling by CO_2 is dominated by wavenumbers near the edges of the CO_2 band (Fig. S1, left). Here, CO_2's mass absorption coefficient falls off roughly exponentially with wavenumber from the center of the CO_2 band (see Fig. 2 in the main text) such that the number of wavenumbers near unity optical depth at any given pressure level is largely insensitive to CO_2 concentration. When atmospheric CO_2 rises, any increase in the spectrally-resolved longwave cooling rate is met by an equal and opposite decrease in the spectrally-resolved longwave cooling rate at other wavenumbers. This tropospheric invariance of H_{CO_2} is implied by the results of several studies (e.g., (1–3)), but its connection to the mechanisms which drive CO_2-induced stratospheric cooling is worth making explicit.

2. The cooling-to-space approximation for CO_2

In the main text, we leverage the cooling-to-space (CTS) approximation (section 2 in the main text) to link CO_2-induced stratospheric cooling to the spectroscopy of CO_2. The validity of the CTS approximation is closely tied to the rate at which Planck emission $B(T)$ changes with optical depth τ (4). If $\gamma = \frac{d\ln B}{d\ln \tau}$ is small (on the order of ∼0.1), the CTS approximation is rather strong; as γ increases, the CTS approximation breaks down.

Because CO_2 is well-mixed ($\beta = 2$) and because the lapse rate Γ in the stratosphere is roughly 1.5 km/K, stratospheric emission from the CO_2 band (where $\alpha = \frac{d\ln B}{d\ln T} \approx 4$)changes slowly with optical depth (4):

$$\gamma_{CO_2} = \frac{d\ln B}{d\ln \tau} = \frac{d\ln B}{d\ln T}\frac{d\ln T}{d\ln p}\frac{d\ln p}{d\ln \tau} = \alpha\frac{R_d\Gamma}{g}\frac{1}{\beta} \approx 4\frac{287\text{J/kg/K}(1.5\text{K/km})}{9.8\text{m/s}^2}\frac{1}{2} \approx 0.09 \quad [1]$$

Here, g is the acceleration due to gravity and R_d is specific gas constant for dry air. Eq. 1 suggests the CTS approximation (Eq. 3 in the main text) is a suitable first-order approximation for the local longwave heating rate due to CO_2 in the stratosphere (H_{CO_2}), a finding in line with previous studies (4–6) and validated by direct comparison to line-by-line computations in Konrad (Fig. S2a).

Due to the linearity implicit in the construction of Eq. 1, the validity of the CTS approximation breaks down near temperature inversions like the stratopause and tropopause (Fig. S2a) where contributions from the inter-atmospheric exchange are large (4). However, since changes in CO_2 concentration yield similar changes in temperature above and below these temperature inversions, radiative heating from the surrounding atmosphere is largely invariant to changes in CO_2 concentration q, making Eq. 5 in the main text a good approximation for $\frac{dH_{CO_2}}{d\ln q}$, even at the stratopause and tropopause (Fig. S2b).

3. Linear parameterizations of CO_2's spectroscopy do not capture the magnitude and vertical structure of stratospheric cooling

Commonly, the spectroscopy of CO_2 is simplified using a parameterization in which the log of CO_2's mass absorption coefficient k_{ref} decays linearly with wavenumber ν away from the center of the CO_2 band ν_0:

$$k_{\text{ref}} = k_0 e^{\frac{|\nu-\nu_0|}{l_0}} \quad [2]$$

Here, k_0 is the mass absorption coefficient at the center of the CO_2 band and l_0 is $\ln k_{\text{ref}}$'s decay rate in wavenumber space. Such parameterizations have been useful in understanding how CO_2 affects tropospheric longwave cooling (1), hydrological sensitivity (7), and the top-of-atmosphere radiation budget (2, 3, 8). However, parameterizing k_{ref} in this manner fails to fully capture the rate at which k_{ref} decays with ν near the center of CO_2 band (Fig. 2c in the main text), causing CO_2's Goldilocks fraction $l = \int_0^\infty \tau_\nu e^{-\tau_\nu} d\nu$ to fall off rapidly with k_{ref}. This transition is particularly sharp when l is approximated using a Dirac delta function (as in Fig. 2c in the main text), but is also apparent when Goldilocks fraction is computed explicitly:

$$l(p,q) = \int_0^\infty \tau_\nu e^{-\tau_\nu} d\nu = 2l_0\left(1 - e^{-\tau_0(p,q)}\right) \quad [3]$$

Here, $\tau_0(p,q)$ is the optical depth predicted by Eq. 2 at the center of the CO_2 band for some CO_2 concentration q at some pressure level p. Eq. 6 in the main text reduces to Eq. 3 for $a = 1$ yet has $a = 0.52$ (see parameter values below) when fitted

to the spectroscopy of CO_2 (gray, Fig. 2 in the main text). This indicates that k_{ref} decays with ν more rapidly near the center of the CO_2 than Eq. 2 would predict. As a result, Eq. 2 produces stratospheric cooling that is amplified near this transition and near zero elsewhere (Fig. S3).

4. Stratospheric shortwave heating

In the main text, we state that, other than the influence of temperature broadening, which is typically negligible, stratospheric shortwave heating does not change with CO_2 concentration so long as the concentration of shortwave absorbers remains fixed (9). In our Konrad simulations, we hold ozone and stratospheric water vapor concentrations fixed across all runs and, as a result, stratospheric shortwave heating changes very little with CO_2 concentration (Fig. S4).

5. How the heating rates of ozone and water vapor change with CO_2 concentration

In the main text, we capture the impact of water vapor and ozone on CO_2-induced stratospheric cooling via a simple empirical parameterization (Eq. 10 in the main text):

$$\frac{dH_o}{dT} = C_{\text{strat}} \cos\left(\frac{\pi}{2}\left(\frac{p - p_{\text{strat}}}{p_{\text{tropo}} - p_{\text{strat}}}\right)\right)^2 \quad [4]$$

Here, p_{strat} is the pressure at the stratopause and p_{tropo} is the pressure at the tropopause. The constant C_{strat}, the temperature sensitivity of H_2O and O_3's combined heating rate at the stratopause, is obtained by fitting Eq. 4 to the change in H_o with temperature predicted by simulations in Konrad (Fig. S5). Because Planck emission grows non-linearly with temperature in the ozone and water vapor bands (a property which Eq. 4 is unable to capture), Eq. 4 generally overpredicts $\frac{dH_o}{dT}$ at high CO_2concentration (when stratospheric temperatures are cooler) and underpredicts $\frac{dH_o}{dT}$ at low CO_2concentration (when stratospheric temperatures are warmer). Nonetheless, Eq. 4 is sufficient for our purposes, offering a simple way to capture the damping effect of $\frac{dH_o}{dT}$ on ΔT, at least to first order (see Fig. 4 in the main text).

Because changes in stratospheric temperature induce a similar change in the heating rate of CO_2 as they do the combined heating rate of ozone and water vapor, spectral efficiency $\eta = \frac{dH_{CO_2}}{dT} / \frac{d(H_{CO_2}+H_o)}{dT}$ is order 1/2 across the depth of the stratosphere (Fig. S6a). Near the tropopause, however, spectral efficiency increases rapidly as ozone concentration (and its associated longwave emission) goes to zero. This increases lower stratospheric cooling (particularly at low CO_2 concentration, Fig. 4 in the main text), though only minimally because changes in $l(p, q)$ with CO_2 concentration q also go to zero near the tropopause.

Spectral efficiency also increases with CO_2 concentration; as CO_2 makes up a larger percentage of the total longwave cooling in the stratosphere, changes in temperature induce a larger change in the heating rate of CO_2 (Fig. S6a). Like η, $\alpha = \frac{d \ln B(T,\nu_0)}{d \ln T}$ is roughly constant across the depth of the stratosphere (Fig. S6b), implying that fractional changes in Goldilocks fraction ($\Delta \ln l$) control the vertical structure of stratospheric cooling ΔT. Additionally, despite η's more pronounced q-dependence, stratospheric cooling depends rather weakly on q because α's (and T's) q-dependence is the opposite sign as η's (Fig. S6c). In the absence of any change in longwave cooling by other gases ($\eta = 1$), stratospheric cooling is significantly amplified, with each doubling of CO_2 yielding over 20K of cooling at the stratopause (Fig. S7).

6. Parameter Values

For reference, Table S1 lists all of the spectroscopic parameters used in our idealized models.

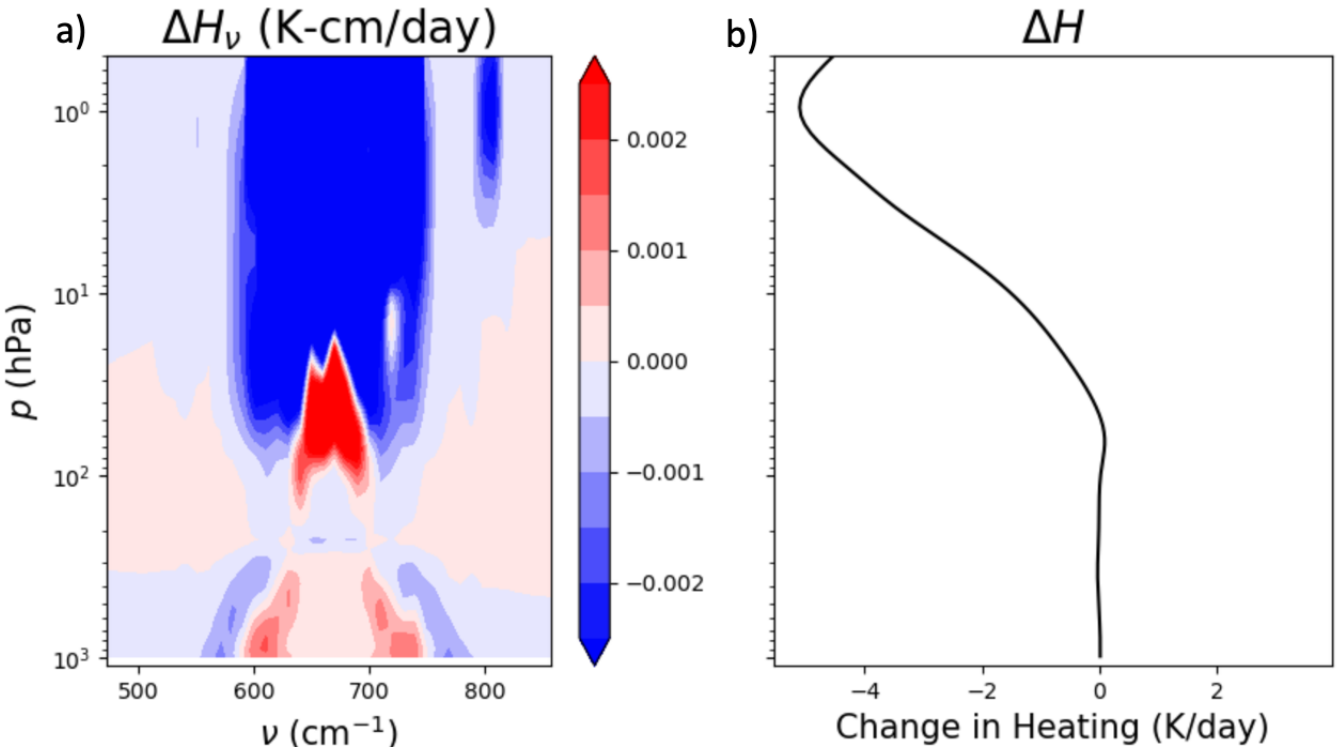

Fig. S1. Spectrally-resolved (a) and spectrally-integrated (b) change in heating across the CO_2 band when CO_2 concentration is quadruped from preindustrial. Temperature is held fixed to the profile which yields radiative convective equilibrium under preindustrial CO_2 concentration (black line in Fig. 1 in the main text).

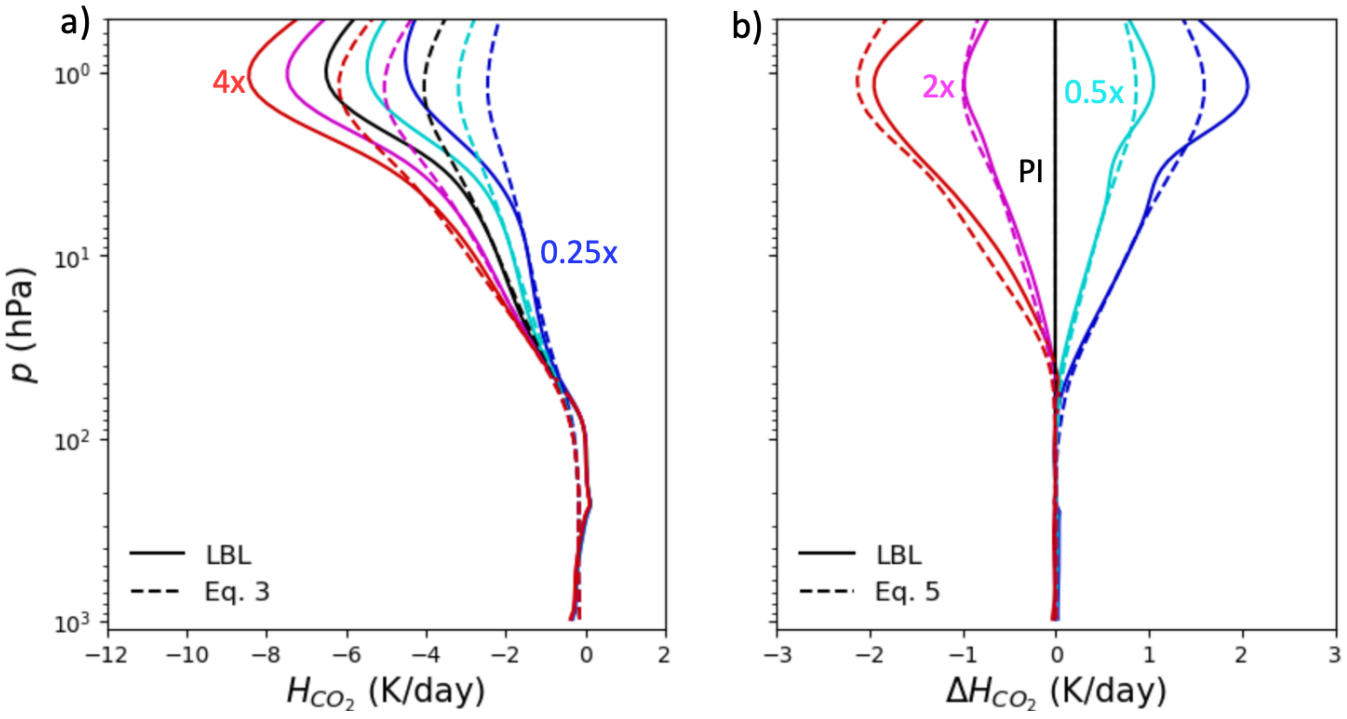

Fig. S2. Heating by CO_2 (a) under preindustrial CO_2 concentration (black) and under subsequent doublings (warmer colors) and halvings (cooler colors) of CO_2 concentration from preindustrial (PI) levels. Line-by-line simulations in Konrad (solid) are compared to Eq. 3 in the main text (dashed), an analytical expression derived using the cooling-to-space (CTS) approximation. The CTS approximation is a suitable first-order approximation for H_{CO_2} in the majority of the stratosphere but breaks down near temperature inversions like the stratopause and tropopause. However, because changes in CO_2 concentration yield similar changes in temperature above and below these temperature inversions, the CTS approximation (Eq. 5 in the main text) generally captures the change in heating by CO_2 with CO_2 concentration (b, same colors and line types) near the stratopause and tropopause.

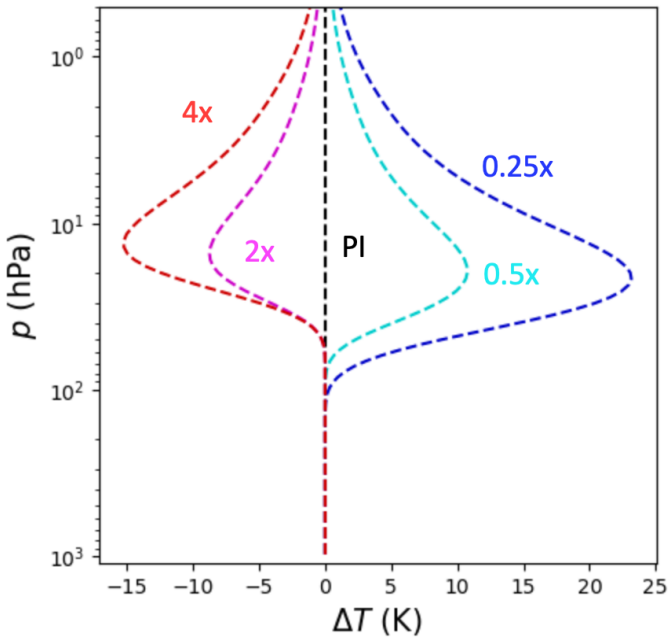

Fig. S3. Stratospheric temperature change from preindustrial conditions (black) under subsequent doublings (warmer colors) and halvings (cooler colors) of CO_2 concentration implied by the linear parameterizations of of CO_2's spectroscopy (Eq. 2). Due to the sharp transition in Goldilocks fraction, stratospheric cooling is amplified near $\tau_0(p, q) = 1$ and near zero elsewhere.

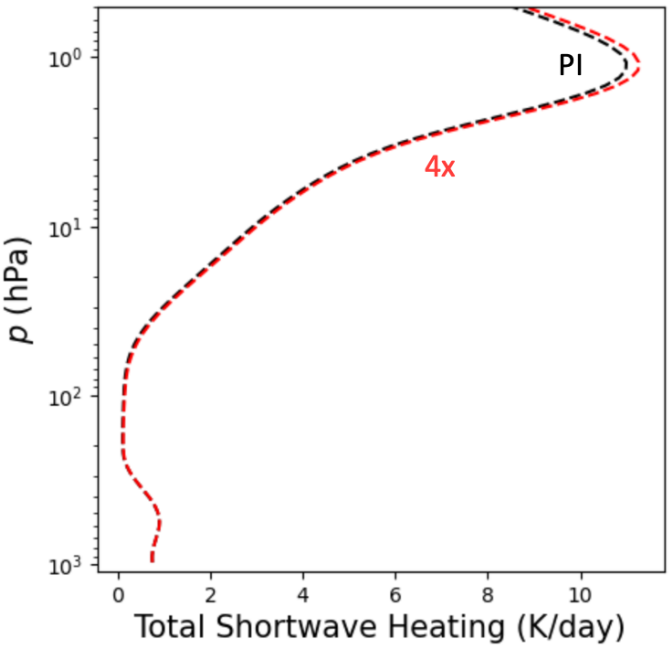

Fig. S4. Spectrally-integrated shortwave heating rate under preindustrial CO_2 concentration (black) and after a quadrupling of CO_2 from PI (red). To first order, shortwave heating is invariant to changes in CO_2 concentration.

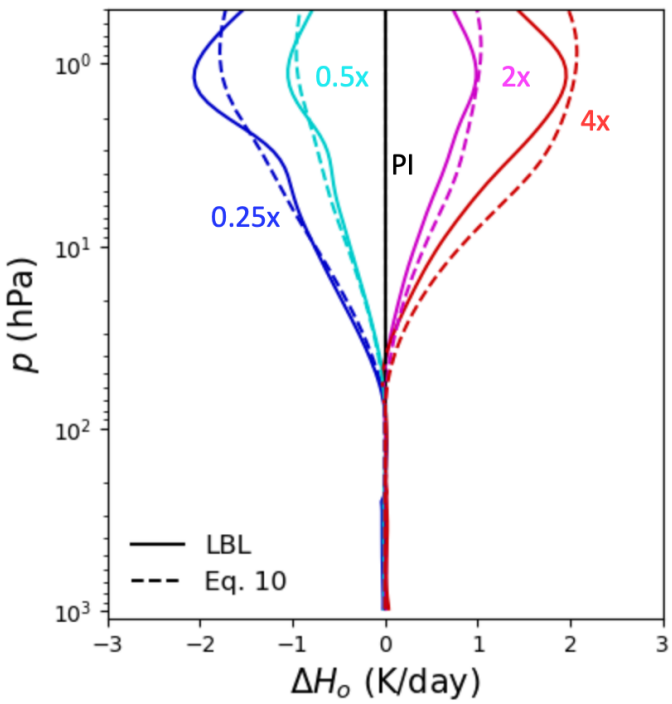

Fig. S5. Change in water vapor and ozone's spectrally-integrated heating rate ΔH_o from preindustrial CO_2 concentration (black) under subsequent doublings (warmer colors) and halvings (cooler colors) of CO_2 concentration. We compare our idealized model (dashed, Eq. 4) to RCE simulations in Konrad (solid).

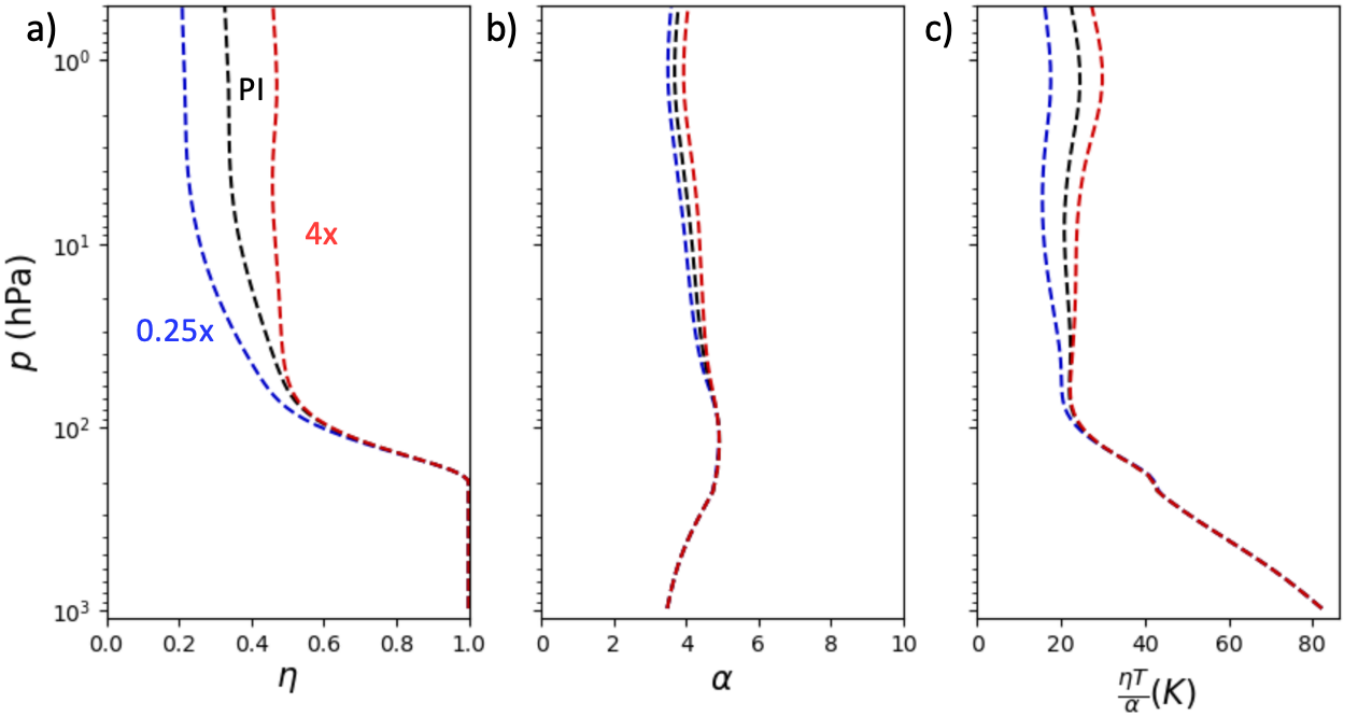

Fig. S6. Spectral efficiency $\eta = \frac{dH_{CO_2}}{dT} / \frac{d(H_{CO_2}+H_0)}{dT}$ (a), source scaling $\alpha = \frac{d \ln B(T,\nu_0)}{d \ln T}$ (b), and the combined effect of these quantities on stratospheric cooling $\frac{\eta T}{\alpha}$ (c) across the depth of the stratosphere for preindustrial CO_2 concentration (black) and for a quadrupling (red) and a quartering (blue) of CO_2 from PI. All quantities are nearly constant throughout the depth of the stratosphere.

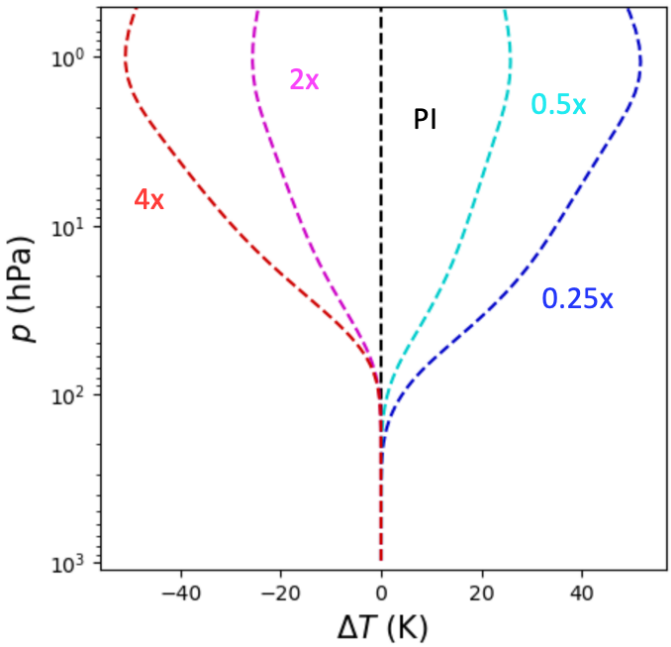

Fig. S7. Stratospheric temperature change from preindustrial conditions (black) under subsequent doublings (warmer colors) and halvings (cooler colors) of CO_2 concentration when longwave cooling by ozone and water vapor is held constant ($\Delta H_o = 0$). Due to the reduced compensation of longwave cooling in other parts of the spectrum, stratospheric cooling is significantly amplified.

Table S1. List of parameters used in our simple model

Parameter	Description	Assumed Value
D	Diffusivity factor	5/3
p_{tropo}	Tropopause pressure level	200 hPa
p_{tropo}	Stratopause pressure level	1 hPa
C_{strat}	Temperature sensitivity of H_2O and O_3's combined heating rate at the stratopause	-0.11 day^{-1}
k_0	Absorption cross-section at which CO_2's Goldilocks fraction begins decaying (at 100hPa)	50 m^2/kg
l_0	Goldilocks fraction at edge of CO_2 band	10.2 cm^{-1}
a	Relative rate at which CO_2's Goldilocks fraction decays with absorption cross-section	0.52
ν_0	Wavenumber of the peak of the CO_2 band	667.5 cm^{-1}

References

1. N Jeevanjee, S Fueglistaler, Simple Spectral Models for Atmospheric Radiative Cooling. *J. Atmos. Sci.* **77**, 479–497 (2020).
2. N Jeevanjee, JT Seeley, D Paynter, S Fueglistaler, An Analytical Model for Spatially Varying Clear-Sky CO2 Forcing. *J. Clim.* **34**, 1–55 (2021).
3. DDB Koll, N Jeevanjee, NJ Lutsko, An Analytic Model for the Clear-Sky Longwave Feedback. *J. Atmos. Sci.* **80**, 1923–1951 (2023).
4. N Jeevanjee, S Fueglistaler, On the Cooling-to-Space Approximation. *J. Atmos. Sci.* **77**, 465–478 (2020).
5. CD Rodgers, CD Walshaw, The computation of infra-red cooling rate in planetary atmospheres. *Q. J. Royal Meteorol. Soc.* **92**, 67–92 (1966).
6. MD Schwarzkopf, SB Fels, The simplified exchange method revisited: An accurate, rapid method for computation of infrared cooling rates and fluxes. *J. Geophys. Res. Atmospheres* **96**, 9075–9096 (1991).
7. S Cohen, R Pincus, A spectroscopic theory for how mean rainfall changes with surface temperature. *Sci. Adv.* **11** (2025).
8. DJ Wilson, J Gea-Banacloche, Simple model to estimate the contribution of atmospheric co2 to the earth's greenhouse effect. *Am. J. Phys.* **80**, 306–315 (2012).
9. S Pinnock, MD Hurley, KP Shine, TJ Wallington, TJ Smyth, Radiative forcing of climate by hydrochlorofluorocarbons and hydrofluorocarbons. *J. Geophys. Res. Atmospheres* **100**, 23227–23238 (1995).